Factors Affecting Ionicity in All-Silica Materials: A Density Functional Cluster Study

Martijn A. Zwijnenburg,[†] Stefan. T. Bromley,*[,†] Christian van Alsenoy,[‡] and Thomas Maschmeyer[†]

Laboratory of Applied Organic Chemistry and Catalysis, DelftChemTech, Delft University of Technology, Julianalaan 136, 2628 BL Delft, The Netherlands, and Structural Chemistry Group, Department of Chemistry, University of Antwerp (UIA), Universiteitsplein 1, B-2610, Antwerpen, Belgium

Received: February 27, 2002; In Final Form: October 4, 2002

Atomic charge analysis is performed on the basis of electron densities obtained from systematic density functional (DF) cluster calculations on structural fragments from seven different all-siliceous zeolites and two all-silica minerals. Charges and ionicities for these fragments are calculated using three different charge analysis schemes: Mulliken, Hirshfeld, and Bader methods. The dependency of the ionicty of the Si−O bond on geometric parameters of the clusters is investigated and it is demonstrated that a correlation exists between the Si−O bond length and its ionicty. Ionicities derived from Bader atomic charges were shown to have a trend opposite to that of ionicities derived from Mulliken and Hirshfeld charges. A simple model is proposed to account for these differences, demonstrating that these opposing trends may be reconciled. The results also suggest a possible link between Si−O bond ionicity and the energetic stability of the corresponding bulk silica polymorph.

Introduction

All-silica crystalline structures consist of repeating patterns of corner sharing SiO_4 tetrahedra, spanning a uniquely large spectrum of different polymorphs and framework densities. Near the lower end of the density range numerous porous materials can be found, which are generically known as zeolites. In zeolites, the regular nanosized channels, threading throughout the crystal, are often large enough for the passage of small molecules. This gives zeolites unique properties, which allow for their advantageous applications as adsorbents, molecular sieves, and catalysts, making use of their characteristic pore size range, framework flexibility, and the adsorption characteristics of the molecules located within the internal pore volume of each zeolite.[1] At the opposite end of the density spectrum reside the many all-silica minerals the study of which is of great importance in the understanding of geological/geochemical processes[2] and which also have applications in optical and microelectronic devices.[3] The bulk physical properties of all of these materials are intrinsically related to a common fundamental property, i.e., the stability of the individual Si−O bonds, holding the system together. This, in turn, is strongly intertwined with the degree of ionicity/covalency of these bonds. The degree of ionicity/covalency of a bond can be defined simply in terms of atomic charges alone.[4] However, such charges are, in fact, particularly difficult to obtain.

Bonding in all-silica materials is traditionally thought of as largely covalent;[5] quartz for example often being treated as a super-molecular structure. However, this view contrasts somewhat with the successes of modeling such systems via the use of interatomic potentials; these models are, with few exceptions, charge-localized ionic methods. Such force-field approaches have given atomic-scale insight into the properties of all-silica zeolites and have further demonstrated that Si and O atomic charges, the resulting ionicities of the Si−O bonds and also the resulting electrostatic potential in the crystal are important in understanding the properties of zeolites.[6,7] Examples of properties, which are influenced by the atomic charges, include the heat of adsorption of various molecules on the Si/O sites, the reactivity of the molecules adsorbed (induced by framework/molecule polarization) and possibly the stability of different zeolite polymorphs (due to the long range of the electrostatic interactions).

The determination of good force-field parameters requires accurate charge information and is typically achieved by fitting to experimental data (e.g. infrared spectra) and/or from electronic structure calculations. In neither case, though, should we expect the resulting atomic charges to accurately mirror the physical charge distribution. In the first case, force fields employ simple point charges to represent the diffuse electron cloud of an atom and generate the further complexity of interatomic bonding via additional parametrized interactions (e.g., bond bending, shell, and torsional terms). This takes much away from the importance of the purely electrostatic term and the match with experiment is a combined fit of many terms. The resulting point charges derived may, thus, have little bearing on the charge distribution of the actual system. More fundamentally, in the case where an accurate model of the charge density is available, such as from a high-level density functional theory (DFT) calculations, the derivation of physical atomic charges is an ill-posed question with numerous possible answers.

Atomic charges, like any other atom-in-a-molecule property, cannot be calculated directly from quantum mechanics[8] since the Schrödinger equation for a molecule (or crystal) makes no reference to the constituent atoms. It is thus impossible to extract objective information about atomic charges from electronic structure calculations. Any method to obtain charges thus consist of partitioning a direct observable and requires an additional assumption about the partitioning method. As a result any

* Corresponding author. Fax: +31-15-2784289. E-mail: S. T.Bromley@tnw.tudelft.nl.
[†] Laboratory of Applied Organic Chemistry and Catalysis.
[‡] Structural Chemistry Group.

10.1021/jp025696s CCC: $22.00
Published on Web 11/27/2002

method to obtain charges is nonunique and its merits can only be assessed in terms of its chemical sensibility and the way it predicts values of observables such as the molecular dipole constant. Because of this lack of a unique definition, a multitude of methods for calculating atomic charges has been developed. Wiberg and Rablen[8] and Bachrach[9] have given an overview of the different methods and their merits.

Previous electronic structure calculations on atomic charges of various all-silica zeolites employing the Mulliken charge partitioning scheme have given charges of between $+1.32|e|$ and $+1.50|e|$ on silicon and between $-0.64|e|$ and $-0.78|e|$ on oxygen using an Hartree−Fock (HF) approach with a STO-3G basis set.[10−12] Using the same methodology, but with a higher-level basis set combination (6-21G for oxygen and 8-31G for silicon), atomic charges between $+2.25|e|$ and $+2.41|e|$ for silicon and between $-1.1|e|$ and $-1.25|e|$ for oxygen were reported.[11,12] Calculations using the higher level DFT method (double numerical with polarization basis set) using Hirshfeld partitioning, applied to various relaxed silica fragments, such as three- and four-membered silica rings, have yielded typical atomic charges of $+0.47|e|$ on silicon and $-0.27|e|$ on oxygen,[13] whereas similar periodic calculations on all-silica Mordenite give typical values of $+0.57|e|$ on silicon and $-0.28|e|$ on oxygen.[14] Atomic charges obtained experimentally by fitting the infrared spectra of α-quartz to a rigid-ion model give ranges between $0.69|e|$ and $1.94|e|$ for the silicon and between $-0.35|e|$ and $-0.97|e|$ for the oxygen atoms.[15−17] Furthermore, it has been also been speculated that the silicon and oxygen atomic charges are functions of the silica geometry.[18]

The results from theory are far from conclusive and suggest that the measure of the ionicity/covalency in all-silica systems has, so far, not found a straightforward answer. The experimental (synthetic) chemistry and physics of SiO_2 materials also suggest that the binding in these system in not clear cut, but has considerable covalent and ionic components.[5] For all-silica zeolites, in particular, further insight into the degree of ionicity of the elemental Si−O bonds could help to understand why the synthesis of pure-silica frameworks seems to be far more difficult than for their deliberately charge-doped aluminosilicate analogues compounds. Tight-binding theory calculations[19] also show that the properties of silica polymorphs can be understood in a model containing, both a covalent and a polar energy term. Because of the relative importance of both terms in all-silica materials, they are also perfect candidate materials to test the various theoretical methods for calculating atomic charges and to probe how they compare with the known properties of such materials.

In high-level studies of all-silica materials and their interactions with adsorbed species, very often the cluster approach is employed. In this way, extended all-silica structures such as zeolites are treated as hydrogen/hydroxyl terminated and/or as embedded silica fragments. This approach implicity assumes a more localized covalent picture of all-silica materials and has been confirmed in its operational validity in many theoretical studies.[20−22] In this paper we employ the cluster approach, using various all-silica structures and cluster sizes to calculate the respective changes in atomic charges and ionicity. The DFT method is used throughout together with Mulliken, Hirshfeld, and Bader (AIM: atoms in molecules) methods for analyzing the resulting charge densities to calculate atomic charges. We compare the ionicities resulting from the different methods via a simple atomic-charge-based comparative measure and examine the effects of geometry, cluster size and basis set on the charges derived.

Computational Methodology. In this paper we investigate three commonly used charge-partitioning methods. First, Mulliken analysis[23] (probably the most widely used method), which simply partitions the charge density derived from the overlap of atomically centered orbitals evenly between the two bonded atoms. Due to the dependence of this method on the atomic orbitals, the size of the basis set used in calculations of electronic bonding characteristics is known to often strongly influence the predicted atomic charges.[8,9] Second, we employ the Hirshfeld[24−26] (or Stockholder) method, which divides the electron density at every point in space between each of the constituent molecular atoms according to a partitioning function, depending on the electron density of the free atoms. Third, Bader's approach is also employed which defines molecular atoms via a topological analysis of the electron density.[27] The latter two methods have been shown to give atomic charges that are relatively basis-set-independent and, in contrast to many other schemes, accurately reproduce physical observables such as molecular dipole moments and electrostatic potentials for small organic and inorganic molecules.[8,25]

It is important to note, however, that although Hirshfeld and Bader analyses seem to perform equally well with respect to predicting properties largely dependent on the magnitude of the atomic charges, the magnitudes of the derived charges in each scheme are quite different. This difference can be understood from the fact that the physical observables predicted in each method are also dependent on higher order multipoles of the electron density, in particular on the atomic dipoles. It is found that for each method the relative magnitude, and thus importance, of the atomic charge term and the atomic dipole term differs considerably. Within Mulliken analysis, in contrast to Hirshfeld and Bader analyses, higher order moments (atomic dipole, atomic quadrupole, etc.) of the bonded atoms cannot be easily defined.[8] Within this investigation, we concentrate on how the various charge-partitioning methods differ regarding their ability to describe a bonded system *solely* in terms of an atomic charge interpretation. For a clear description of ionicity/covalency, concepts based on atomic charges, a method which models a system most appropriately and accurately at the single charge/monopole level is to be preferred over those methods requiring higher order moments. Such a description would, to the first order, give the most concise and chemically intuitive assessment of the charge distribution, the ionicity/covalency and, thus, the chemistry of a system.

In this study, we employ a cluster approach to investigate a collection of known all-silica polymorphs. For each extended structure a comparative fragment of 16 atoms (Si_4O_{12}), was used, in each case consisting of a ring of four oxygen atoms and four silicon atoms with two further oxygen atoms bonded to each silicon atom in the ring. Such four-rings are a good representative silica model being present in almost 90% of all zeolite frameworks, in various denser crystalline forms of silica and also within amorphous glassy silicas. To saturate the dangling oxygen bonds of each four-ring, eight hydrogen atoms were placed at an appropriate bond length of 0.98 Å[28] in the direction of the missing O−Si bond from the respective periodic structure. This method of cluster termination has been widely and successfully used in the modeling of extended silicas[20−22] and owes much of its utility to the electronegativity of hydrogen lying between that of silicon and oxygen. In such a treatment, however, it is essential that the terminating hydrogens are not permitted to relax in any subsequent calculation as this is very likely to result in surface reconstruction effects, e.g., the

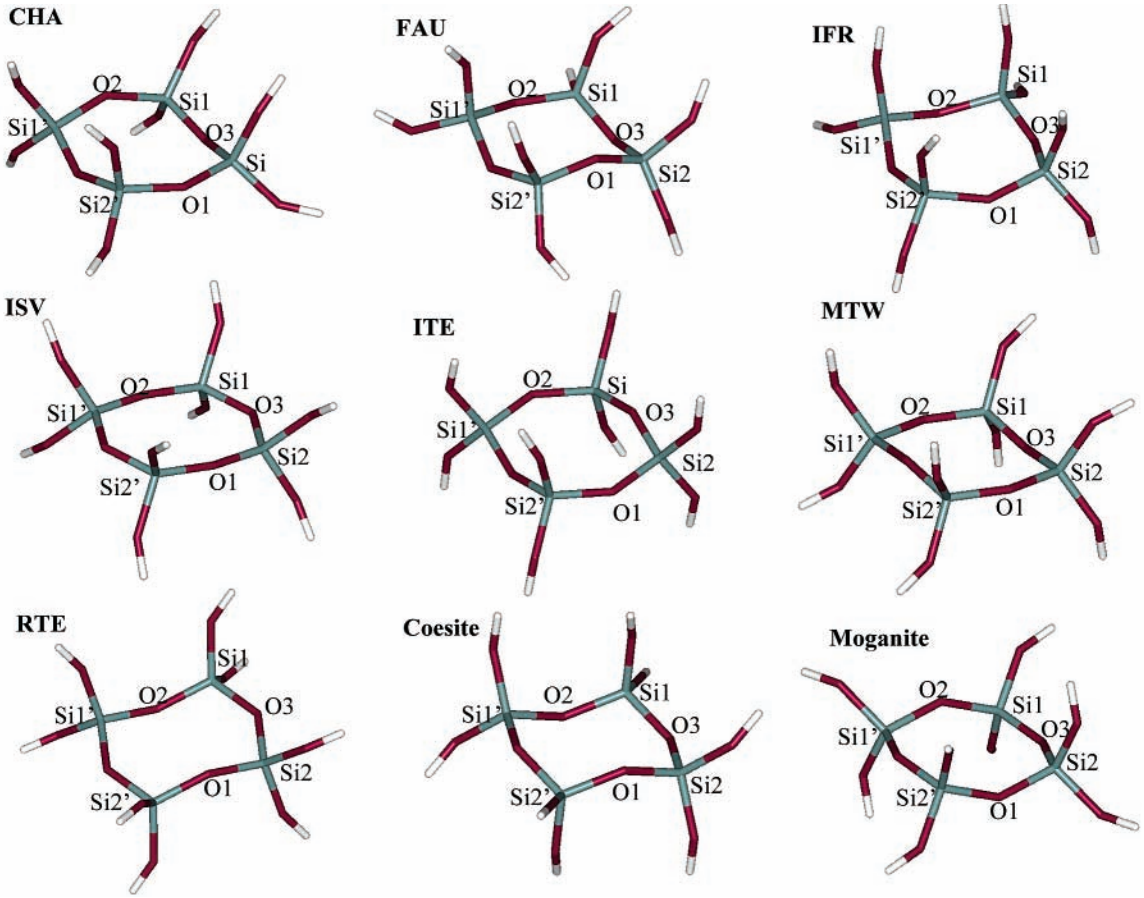

Figure 1. Four-ring fragments used in the calculations. The labels indicate the respective crystal structure from where the fragments were taken.

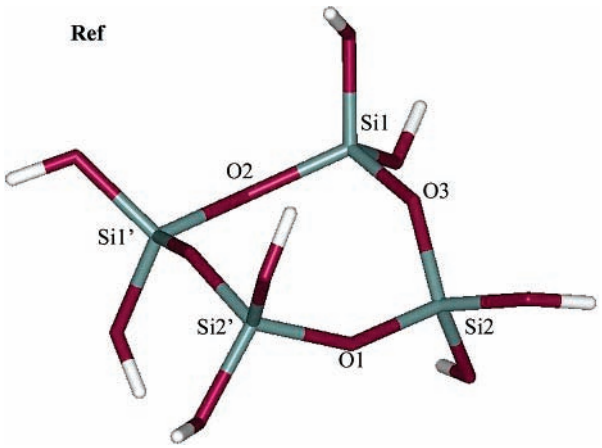

Figure 2. Reference four-ring silica fragment used in calculations obtained from free-space DFT optimization.

formation of intramolecular hydrogen bonds, which will destroy the role of the hydrogen atom as an approximate bulk-silicon embedding-atom and thus also mask any meaningful results.[14] Although fixing the hydrogens, the relaxation of the remainder of the silica is optional and advocated by some authors.[29] In our study however, we wish to compare experimentally determined structures and thus use the respective published coordinates for each material investigated. As a reference system for these structures, a free-space silica four-ring, optimized at a high level of DFT theory was used, see Figure 2. Optimization of a free-space silica four-ring using the Gaussian 98 code, was, as expected, found to always yield a hydrogen-bonded conformation.[13] A preferred reference system was taken to be the non-hydrogen-bonded silica four-ring recently described by Pereira et al.,[13] also obtained as a valid minimum structure via high-level DFT optimization. This silica four-ring, displayed in Figure 1, is preferred over the slightly lower energy hydrogen-bonded four-ring, as it more accurately mimics the fully connected silica rings found in all-silica structures, having no internal hydrogen bonds.

The cluster approach was preferred over periodic calculations due to practical and methodological reasons. First, the cluster approach allowed us to study a relatively large number of materials at a high DFT level of theory. To conduct such high level calculations periodically for every one our structures would have been computationally prohibitively expensive at present. As a bulk comparison of our methodology it is possible to perform fully periodic DFT calculations of some small unit cell structures such as CHA,[30] though often with assumptions of high symmetry to reduce the experimentally determined unit cell size. Such calculations are only of use if the same level of theory can be employed in the periodic case as in the cluster calculations. In practice periodic DFT codes traditionally use plane wave basis sets, which are difficult to compare with our Gaussian basis sets employed. With some codes however such a calculation may be possible although here it is found that basis sets including polarization functions suitable for accurate silica cluster calculations are often not readily transferable to the corresponding periodic calculation. In addition to the problems of comparison of the calculation details, the three methods of charge analysis open to us i.e., Mulliken, Hirshfeld, and Bader, for molecular systems, are not, to our knowledge, all currently simply available in a single periodic DFT code. Furthermore, it has been shown in numerous previous studies[20−22,31] that silica clusters with suitably fixed terminating hydrogens are very good models of extended all-silica solids.

TABLE 1: Geometry of Silica Four-Rings[a]

	Si1−O2	Si1−O3	Si1−nOU	Si1−OD	Si2−O1	Si2−O3	Si2−OU	Si2−OD	Si1−O2- Si1′	Si1−O3−Si2	Si2−O1−Si2′
ref	1.610	1.603	1.599	1.599	1.599	1.603	1.611	1.599	147.5	145.8	150.7
CHA	1.597	1.607	1.604	1.614	1.604	1.607	1.597	1.614	149.4	138.4	145.8
FAU	1.616	1.594	1.570	1.557	1.622	1.619	1.572	1.619	143.5	145.1	149.3
IFR	1.563	1.559	1.661	1.661	1.563	1.559	1.661	1.661	166.1	134.8	166.1
ISV	1.625	1.625	1.622	1.625	1.625	1.624	1.624	1.623	148.1	154.7	148.1
ITE	1.546	1.587	1.584	1.555	1.591	1.660	1.543	1.593	156.2	158.6	156.2
MTW	1.612	1.629	1.613	1.624	1.615	1.630	1.620	1.610	156.9	139.2	156.9
RTE	1.642	1.650	1.649	1.650	1.642	1.654	1.645	1.652	148.6	142.8	148.6
coesite	1.607	1.631	1.598	1.598	1.619	1.617	1.608	1.625	145.0	136.1	145.0
moganite	1.610	1.614	1.610	1.614	1.612	1.605	1.591	1.612	145.0	145.8	145.0

[a] All distances in angstroms. All angles in degrees. OU = terminating oxygen above the plane of the ring. OD = Terminating oxygen below the plane of the ring.

TABLE 2: Atomic Charges for Each of the Four-ring Fragments[a]

	Si1			Si2			O1			O2			O3		
	Q_M	Q_H	Q_B	Q_M	Q_H	Q_B	Q_M	Q_H	Q_B	Q_M	Q_H	Q_B	Q_M	Q_H	Q_B
ref	1.117	0.513	3.262	1.110	0.512	3.265	−0.619	−0.296	−1.647	−0.619	−0.296	−1.647	−0.634	−0.314	−1.662
CHA	1.070	0.501	3.326	1.081	0.509	3.326	−0.535	−0.281	−1.658	−0.575	−0.307	−1.671	−0.562	−0.300	−1.670
FAU	1.105	0.511	3.320	1.078	0.503	3.321	−0.578	−0.305	−1.675	−0.541	−0.287	−1.661	−0.575	−0.296	−1.661
IFR	1.056	0.489	3.341	1.094	0.506	3.322	−0.596	−0.320	−1.668	−0.590	−0.319	−1.672	−0.562	−0.300	−1.663
ISV	1.020	0.519	3.308	1.020	0.519	3.308	−0.476	−0.262	−1.689	−0.476	−0.262	−1.689	−0.440	−0.257	−1.649
ITE	1.119	0.509	3.310	1.120	0.514	3.308	−0.583	−0.304	−1.661	−0.583	−0.304	−1.661	−0.593	−0.313	−1.670
MTW	0.971	0.484	3.355	1.047	0.512	3.332	−0.488	−0.288	−1.677	−0.488	−0.288	−1.677	−0.585	−0.322	−1.671
RTE	1.106	0.511	3.311	1.114	0.512	3.314	−0.567	−0.276	−1.660	−0.567	−0.276	−1.660	−0.599	−0.314	−1.655
coesite	1.133	0.500	3.325	1.095	0.503	3.315	−0.590	−0.300	−1.669	−0.590	−0.300	−1.669	−0.600	−0.316	−1.655
moganite	1.077	0.502	3.313	1.099	0.509	3.314	−0.584	−0.295	−1.657	−0.584	−0.295	−1.658	−0.565	−0.296	−1.663

[a] Q_M is the Mulliken atomic charge, Q_H the Hirshfeld atomic charge, and Q_B the Bader atomic charge. (6-31G* basis set).

To correct for the absence of long-range interactions in silica cluster calculations without using periodic methods, hybrid quantum mechanical/molecular mechanical (QM/MM) schemes are commonly applied. Such schemes often only treat the steric interactions of the immediate crystalline environment of the silica cluster,[32] which, since we are taking fixed experimental geometries would, by definition, be of no benefit in our study. Other schemes are able to further incorporate the long-range electrostatic field,[33] and in some cases also polarization effects of the bulk crystal.[34] These latter embedding schemes, however, need values for the point charges around the cluster fitted to reproduce the long range Madelung field of the bulk material. To efficiently estimate the Madelung field a periodic calculation is required beforehand, usually at a lower level of theory than that used for the embedded cluster, e.g., suitable interatomic potentials,[34] or Hartee−Fock calculations.[33] According to this prescription of forming the point charge embedding shell the charge values are by necessity fitted to a less accurate, or at best different, description of the electrostatic bulk environment than that of the local environment of the embedded cluster itself. In the case of using charges from interatomic potentials, in particular, for calculating the embedding environment, we would in fact presuppose the very thing we are trying to ascertain in this study, i.e., the atomic charges of the silicon and oxygen atoms. Although we are conscious of the need for a better description of the electrostatic environment for more accurate calculations, we feel that the main contribution of such long-range effects is on the total energy rather than on local properties such as the bonding and thus the charge distribution, which are rather more influenced by geometric and electronic factors. To demonstrate how the partitioned charges change with a fuller account of the bulk environment we have also performed calculations on significantly larger clusters taking into account of the order of 60 further atoms of the silica bulk material atoms around the respective 16 atom four-ring cluster. As we show later the corresponding partitioned charges from our 16 atom clusters shift by a small consistent percentage when going to the larger embedded clusters leaving our conclusions, based on ionicity trends, unchanged. Furthermore, as judged by published periodic calculations,[14] the atomic charges in our larger clusters seem to have already saturated at typical bulk values.

All clusters, with exception of the reference four-ring, were obtained from crystal structure refinements of all-silica materials (indicated for zeolites by the reference code of their framework types: CHA,[35] FAU,[36] IFR,[37] ISV,[38] ITE,[39] MTW,[40] RTE,[41] Coesite,[42] Moganite[43]). [The powder diffraction derived crystallographic data for the all-silica form of MTW has relatively large R-factors and a large range of Si−O bond lengths, making the structural parameters less reliable. The respective MTW data is, thus, highlighted in each plot.] Geometric details of the different silica four-rings can be found in Table 1. The DFT calculations were performed using the three-parameter B3LYP[44,45] hybrid functional, as implemented in the program Gaussian 98.[46] Various basis sets, 3-21G;[47−51] 6-31G,[47,48] 6-31G*,[47,48] and 6-31G**[47,48] were employed to study the effect of the basis set on the result of the calculations. Mulliken charges were obtained from the Gaussian 98 code, Hirshfeld atomic charges were calculated using the Stock program,[25] and Bader (AIM) charges were calculated via the AIM2000 program.[52]

Results

The charges calculated for all independent atoms in each four-membered silica ring are shown in Table 2 and were used in the calculation of ionicities in all reported graphs unless stated otherwise. All results presented are obtained via single point DFT calculations. The ionicity measure employed between two bonded atoms A and B is derived from the respective calculated Mulliken, Hirshfeld or Bader atomic charges via the equation

$$\kappa_{A-B} = \frac{1}{2}\left|\left(\frac{Q_A}{\nu_A}\right) - \left(\frac{Q_B}{\nu_B}\right)\right|$$

given in.[4] Q_A is the atomic charge of atom A and ν_A is the valence of atom A. It should be noted that this measure of ionicity is dependent only on the magnitudes of the atomic charges, in line with chemical intuition of this concept. This

TABLE 3: Basis Set Dependency for the ITE Four-Ring

		Si1	Si2	O2	O3
3-21G	Q_M	1.665	1.660	−0.900	−0.925
	Q_H	0.588	0.591	−0.346	−0.358
	Q_B	3.387	3.379	−1.719	−1.738
6-31G	Q_M	1.715	1.703	−0.917	−0.949
	Q_H	0.584	0.588	−0.312	−0.354
	Q_B	3.228	3.218	−1.632	−1.653
6-31G*	Q_M	1.119	1.120	−0.583	−0.593
	Q_H	0.509	0.514	−0.304	−0.313
	Q_B	3.310	3.308	−1.661	−1.670
6-31G**	Q_M	1.115	1.118	−0.581	−0.591
	Q_H	0.512	0.517	−0.304	−0.312
	Q_B	3.311	3.308	−1.663	−1.672

definition of ionicity, as opposed to other possible ionicity measures,[27] allows us to directly compare various atomic charge-partitioning schemes on an equal footing. The variation in ionicity for a range of all-silica clusters of different geometries and sizes, employing different basis sets and charge partitioning methods is reported below. In each case only the central ring silicon and oxygen atoms of each cluster were used to calculate the ionicities (i.e., oxygen atoms with a directly bonded hydrogen were not included). This choice of atoms better reflects the environment of the atoms in the O−Si−O and Si−O−Si embedded atoms found in the corresponding extended all-silica zeolites.

Basis-Set Dependency. Mulliken, Hirshfeld, and Bader atomic charges calculated over the central silicon and oxygen atoms of an ITE four-membered ring are given in Table 3. The charges were calculated using the electron density obtained from the DFT calculations for a series of four different basis sets (3-21G, 6-31G, 6-31G*, and 6-31G**). The trends observed for the ITE silica ring were found to be representative of all silica clusters calculated.

The first point to note is the marked difference between the three different charge-partitioning methods in the magnitude of the predicted charges of the silicon and oxygen atoms. All methods give the same sign of the charge for the corresponding atom type, but the Mulliken charges are between 2 and 3 times larger than the Hirshfeld atomic charges, and the Bader charges, in turn, over twice as big as the Mulliken charges depending on the basis set used.

The Mulliken charges are, as expected from literature,[8,9] strongly dependent on the basis set used in the calculations, decreasing on average by $0.55|e|$ (−33%) and $0.33|e|$ (−36%) for the silicon and oxygen charges from the smallest to the largest basis set description. From the silicon/oxygen charge balance, it may be expected that this change in absolute magnitude of the atomic charges should be equal in both cases, thereby, maintaining charge neutrality. However, there is a moderate difference since the terminal hydroxyl groups are not included in this charge balance.

The Hirshfeld and Bader charges are much less sensitive to the choice of basis sets, inclusion of polarization functions on the silicon and oxygen atoms having a small, yet still marked effect. The silicon and oxygen charges decrease each by a similarly modest amount $0.07|e|$ (−13%) and $0.04|e|$ (−12%) for Hirshfeld, and $0.07|e|$ (−2%) and $0.06|e|$ (−4%) for Bader, respectively, when going from the smallest to the largest basis set. For all schemes, the largest component in this overall change arises when going from a nonpolarization basis set description (3-21G/6-31G) to basis sets where d polarization functions are included on all the silicon and oxygen atoms (6-31G*). The effect of also adding an extra p function to the terminating hydrogen atoms has relatively little influence on the predicted central ring atomic charges. The effect of polarization functions on calculated atomic charges has been described previously[8,25] and is caused by the extra spatial degrees of freedom for the electron density introduced by the d-functions, giving a better description of the Si−O bond. This is especially true for the relatively larger, more polarizable, oxygen-centered electron density. The treatment of oxygen as a polarizable species has also been found to be beneficial in classical models of siliceous materials via the use of shell models.[53] The Si−O ionicity κ_{Si-O}, which can be calculated easily from the charges derived from the three different partioning methods, is also found to simply follow the same basis-set-dependent trends observed for the actual charges. Considering the above, the 6-31G* basis set was used in all subsequent calculations.

Finite-Size Effects. Ideally one should use the electron density from fully periodic DFT calculations on the respective zeolite crystals to obtain the atomic charges. However, since calculations on such systems are still extremely demanding computationally, hydroxyl-terminated clusters were used. To estimate the error generated by taking clusters instead of the fully periodic lattice, five larger silica fragments based around a four-ring core were also studied. These clusters differ from the original silica four-membered rings in that every silicon atom in the original ring is now linked to at least one further silicon atom before terminating in a hydroxyl group, giving a second embedding "coordination sphere" around the original rings increasing the number of atoms in the cluster by approximately five times. An example of a larger cluster used, for ITE, can be seen in Figure 3.

Table 4 shows the change in the calculated atomic charges for, both, the original atoms in the four-ring and the relevant atoms in the larger embedded fragment for the both Mulliken and Hirshfeld charge-partitioning methods. The effects of cluster size on the magnitude of the Bader charges is not reported due to the very significant computational expense of the calculations, but is assumed to be similar to the reported small shifts for both Mulliken and Hirshfeld charges. From the tabulated data it can be seen that the calculated atomic charges in the ring, upon increasing the cluster size, are consistently shifted for each partitioning method. This shift however, is found to be rather small being on average $-0.027|e|$ for the oxygen atoms and $0.065|e|$ for the silicon atoms using Mulliken partitioning and $0.052|e|$ and $0.012|e|$, respectively, when using Hirshfeld partitioning. The change in the ionicities calculated from these shifted charges can be examined via the crossed data-points on each graph lying vertically above the data points of the smaller clusters. Importantly, there is little change in going to larger silica clusters in the trends observed for the smaller silica four-rings, showing that the effects of cluster size play little part in determining reliable values of the atomic charges and ionicities, thus, further justifying the chosen cluster approach. This conclusion is further strongly confirmed by comparison with fully periodic DFT calculations on the all-silica form of Mordenite[14] which give Hirshfeld atom charges of $0.57|e|$ on silicon and $-0.28|e|$ on oxygen in excellent agreement with our average large cluster Hirshfeld values of $0.56|e|$ and $-0.28|e|$, respectively, showing that the charges, and thus the derived ionicities, are close to their saturated periodic values for the clusters employed.

Geometric Effects on Ionicity. Previous research has hinted on strong correlations between atomic charges and geometrical parameters of the zeolite.[18] Since atomic charges and ionicities are strongly connected with each other, we will explore the influence of geometry on the ioncity of bonds. The most important local geometric parameters in determining the long-

TABLE 4: Partitioned Atomic Charges for Large Fragments and Charge Difference (ΔQ) between Large and Small Fragments (6-31G* basis set)

		Si1	ΔQ	Si2	ΔQ	O1	ΔQ	O2	ΔQ	O3	ΔQ
Mulliken	CHA	1.121	0.051	1.127	0.046	−0.540	−0.005	−0.606	−0.031	−0.582	−0.020
	FAU	1.158	0.053	1.148	0.070	−0.613	−0.036	−0.549	−0.008	−0.588	−0.013
	ITE	1.150	0.031	1.202	0.082	−	−	−0.609	−0.133	−0.631	−0.037
	MTW	1.071	0.100	1.124	0.077	−0.507	−0.019	−0.507	0.076	−0.628	−0.043
	RTE	1.174	0.068	1.186	0.072	−0.568	−0.002	−0.568	−0.081	−0.631	−0.031
Hirshfeld	CHA	0.562	0.061	0.560	0.051	−0.280	0.001	−0.288	0.019	−0.284	0.015
	FAU	0.558	0.048	0.560	0.057	−0.285	0.020	−0.278	0.009	−0.286	0.009
	ITE	0.558	0.049	0.561	0.047	−	−	−0.289	0.016	−0.291	0.021
	MTW	0.534	0.049	0.562	0.050	−0.279	0.009	−0.279	0.009	−0.300	0.022
	RTE	0.561	0.050	0.565	0.054	−0.278	−0.001	−0.278	−0.001	−0.290	0.025

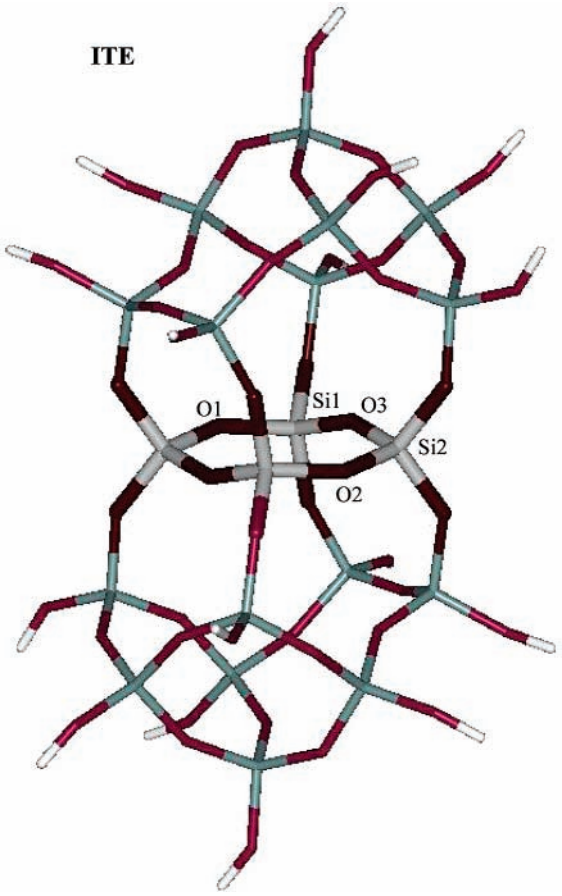

Figure 3. Example of a larger structural fragment (from the ITE structure) used in the finite size calculations. The smaller "embedded" ITE four-ring is highlighted with thicker bonds.

range structure of all-silica materials are generally believed to be strongly linked to the Si−O bond lengths and the Si−O−Si angles. The O−Si−O angles, however, are often assumed to be relatively constant within silicon-centered rigid tetrahedra, a model which has found much success in describing the topologies and physical properties of numerous silica polymorphs.[54,55] Following this proven philosophy, we have derived ioncities of all independent bonds within all the four-membered silica rings (shown in Figures 1 and 2, employing eq 1, using atomic charges calculated from the Mulliken, Hirshfeld and Bader partitioning methods) and calculated the values as a function of both Si−O bond length and Si−O−Si angle.

Figure 4a−c shows how the calculated ionicity varies with Si−O bond length for each of the charge partitioning methods. In each case there is evidence of a strong correlation between Si−O bond length and ionicity of the respective bond. As for the calculated atomic charges (see Table 2), for each charge partitioning scheme the derived ioncities differ considerably in magnitude. It is to be noted that both Hirshfeld and Bader schemes, the best performing partitioning methods with respect to reproducing physical observables, give almost opposite predictions for the ionicity of the Si−O bonds (Bader, ∼0.83; Hirshfeld, ∼0.14). Mulliken analysis gives Si−O ionicities, according to eq 1, of a magnitude between these extremes (∼0.28). Both Hirshfeld and Mulliken methods show an increasing trend in ionicity with increasing Si−O bond length with the ionicities increasing by ∼0.06 and ∼0.035 respectively over the same range of Si−O bond lengths (1.546 Å − 1.660 Å). Over this bond length range, ionicities derived from Bader-partitioned atomic charges show a small decreasing trend of 0.019 in ionicity. It is noted that the trends observed for the silicon charges follow those of the respective ionicity trends.

Unlike the bond length plots, the change in ionicity with respect to the O−Si−O angle showed no discernible strong trends for any of the charge-partitioning methods. No attempts were made to fit the data to a surface as described by Larin et al.[12]

Energy and Ionicity. In Table 5, the total calculated energy of each of the four-membered silica ring fragments and the average ionicity of the respective Si−O bonds within each ring is shown. However, due to the small sample of representative Si−O bonds in each fragment, the reported relative energies do not necessarily reflect the energetic stability of each corresponding bulk silica polymorph. On the other hand, as each finite fragment represents the same structural unit in each polymorph, each four-ring cluster, via its geometry, gives an approximate comparative measure of the global, crystal-morphology-induced distortion away from its fully relaxed state. In this way we can imagine that, for example, that fragments with relatively shorter Si−O bond-length are representations of relatively more compressed global topologies of the host silica material and fragments with longer Si−O bonds are representing more relaxed bulk structures. While a one to one correlation between ioncity and bulk energy is, thus, not to be expected, it is nevertheless interesting to note that for Mulliken and Hirshfeld analyses a tendency is observed for the energy of the fragment to increase with decreasing average ionicity along with the corresponding inverse tendency for Bader derived ionicities (see Table 5). We also compare published experimental heat of formation data[56] to ionicity and see similar, albeit less pronounced, tendencies. The corresponding data for Mulliken and Bader analysis is shown more clearly in Figure 5a,b.

The lowest energy reference structure is the relaxed ring with the majority of the rest of the ring fragments lying between 39.4 and 67 kcal/mol higher in energy. The ISV fragment is found to be, by far, the highest energy structure lying 108.5 kcal/mol above the relaxed four-ring energy. This high energy is probably due to its rather distorted structure (see Table 1), which in turn is probably due to it being part of a unique double-four-ring strained configuration within the zeolite crystalline

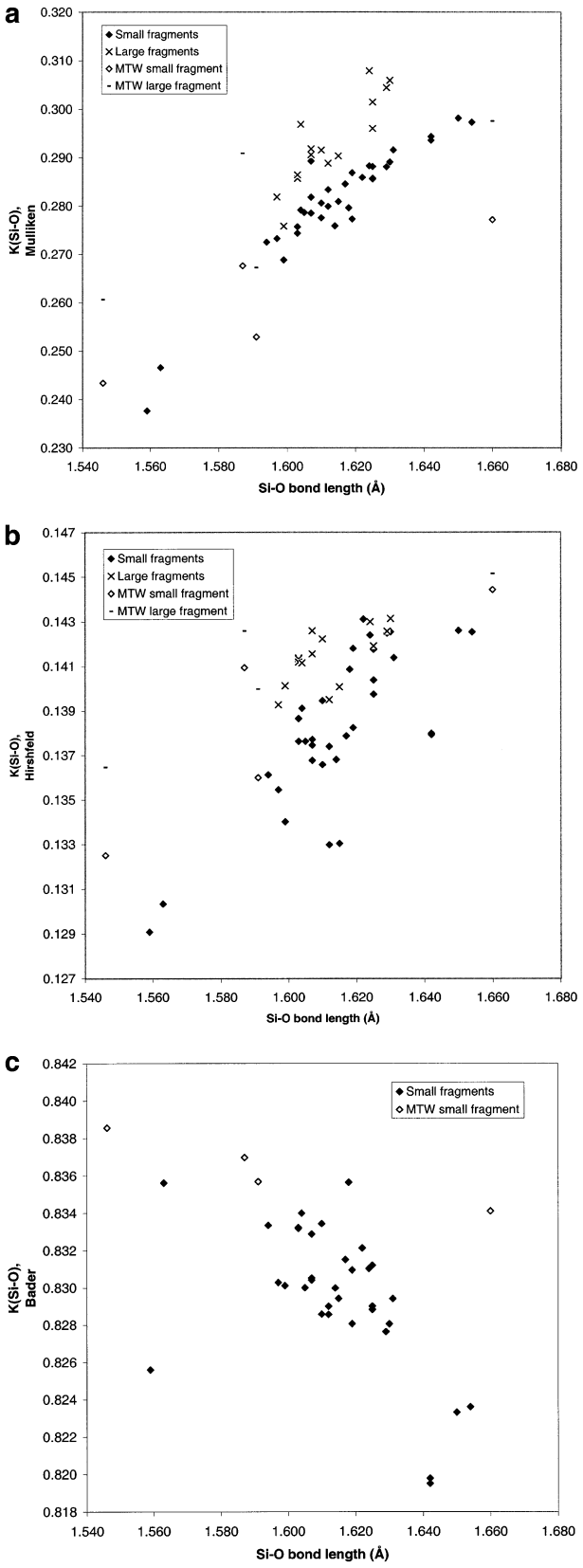

Figure 4. a. Calculated Mulliken ionicities verses Si−O bond length for the four-ring fragments. The crossed datapoints indicate the finite size shift in ionicity, each lies vertically above its respective smaller fragment ionicity data point. b. Calculated Hirshfeld ionicities verses. Si−O bond length for the four-ring fragments. c. Calculated Bader ionicities verses Si−O bond length for the four-ring fragments.

ISV structure. The MTW structure is also found to be relatively high in energy with respect to the relaxed four-ring, which may again be indicative of some inaccuracies in the powder diffraction crystal structure.

Laplacian at the Bond Critical Point. An alternative measure of ionicity is the Laplacian of the electron density at the bond critical point ($\nabla^2\rho_{(rc)}$) as defined by Bader[27] and commonly used in the understanding of bonding in minerals.[57,58] Negatively valued Laplacians are indicative of covalent interactions while positive Laplacians are characteristic of closed-shell (ionic, van der Waals) or "intermediate" type of interactions. Figure 6 shows the variation of $\nabla^2\rho_{(rc)}$ with Si−O bond length. Normally this type of information is obtained from densities calculated with computationally relatively uneconomical basis sets (6-311++G**). Our test calculations have show that the errors in $\nabla^2\rho_{(rc)}$, when going from a 6-311++G** to a 6-31G* basis set, are smaller than 10% for our system and, thus, the smaller basis sets is used throughout. The insert to Figure 6 shows that there is a correlation between $\nabla^2\rho_{(rc)}$ and the calculated Hirshfeld ionicity. That such a correlation is shown to exist indicates that both yardsticks describe the same phenomena.

Discussion

As reviewed in the Introduction, the degree of ionicity/covalency of silica materials has been subject to much discussion and speculation due to its fundamental role in the understanding, modeling and practical application of such materials. One of the prime reasons for the lack of clarity in this debate, is due to the fact that different analysis methods give often conflicting results. From the result of our DFT calculations, Mulliken and Hirshfeld analysis give small atomic charges and equally moderate ionicities, reminiscent of a mainly covalent material with a minor ionic component in the bonding. Bader's atom-in-molecule analysis on the other hand predicts nearly fully charged silicon and oxygen ions and ioncities exceeding 80%, being characteristic of a "classical" ionic solid. Along with these striking differences in the calculated magnitudes of the atomic charges and ionicities for each of the partitioning methods, it is also found that the range of the predicted values for each measure differs considerably.

When comparing our calculated ionicities for each partitioning scheme against variations in the Si−O bond length, correlations were found. For both Mulliken and Hirshfeld analysis we see a tendency for the ionicity to increase with increasing Si−O bond length. Bader analysis on the other hand shows a decrease of ionicity with increasing Si−O bond length. In a previous study by Larin et al.,[11] using Mulliken analysis with a periodic HF approach on a set of all-silica zeolite structures, a decrease in the silicon charge with an increase in average Si−O bond distance was observed. This would imply that the calculated ionicity would decrease with increase in Si−O bond length in contrast to our Mulliken-based ionicity trend. This difference could be due to a number of factors, but is likely to be due to the contrasting calculation methods and the zeolite structures employed. The DFT methodology employing in this work, although generally of a higher quality than the HF calculation approach vide supra should not give significantly different electronic densities and has been independently tested by us via a series of cluster HF calculations. The effect of using a cluster rather than a periodic structure has also been validated, with our finite size cluster calculations showing that our larger charge-saturated clusters give the same trends in the ionicties, and only consistent small shifts in atomic charge magnitudes, with respect to our smaller clusters. One rather large and important difference, though, is the size of the basis set

TABLE 5: Total Energy of the Cluster and Experimental Relative Framework Enthalpy[48] versus Average Cluster Ionicity (6-31G* basis set)

	total energy (Ha)	relative energy (kcal/mol)	average ionicity, κ_{Si-O}			ΔH^{298}_{trans} (kcal/mol)
			Mulliken	Hirshfeld	Bader	
4-RING	−2066.23428	0.00	0.296	0.140	0.822	-
Moganite	−2066.17144	39.40	0.280	0.137	0.829	0.81
ITE	−2066.15765	48.05	0.287	0.141	0.830	2.41
FAU	−2066.15711	48.39	0.278	0.137	0.831	3.25
RTE	−2066.15481	49.83	0.285	0.138	0.829	-
CHA	−2066.14410	56.55	0.274	0.137	0.832	2.72
Coesite	−2066.13648	61.33	0.288	0.140	0.830	0.70
IFR	−2066.12894	66.06	0.279	0.140	0.833	2.39
MTW	−2066.12738	67.04	0.260	0.138	0.836	2.08
ISV	−2066.06126	108.50	0.242	0.130	0.831	3.44

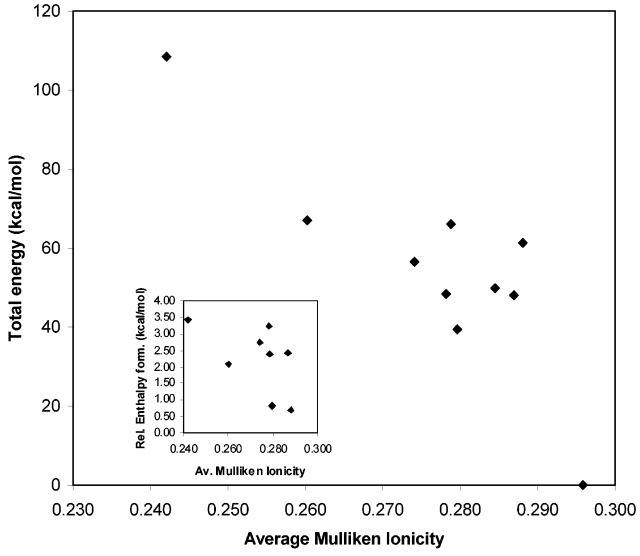

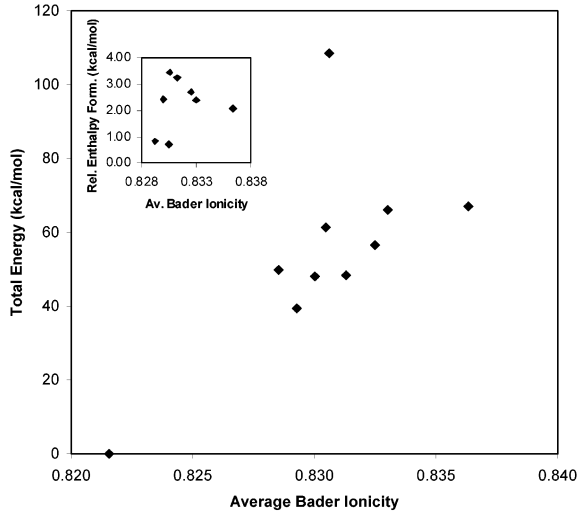

Figure 5. a. Average Mulliken ionicities verses total calculated energy of the fragments (inset shows average Mulliken ionicity verses experimental heat of formation data[48] for all-silica crystals). b. Average Bader ionicities verses total calculated energy of the fragment (insert shows average Bader ionicity verses experimental heat of formation data[48] for all-silica crystals).

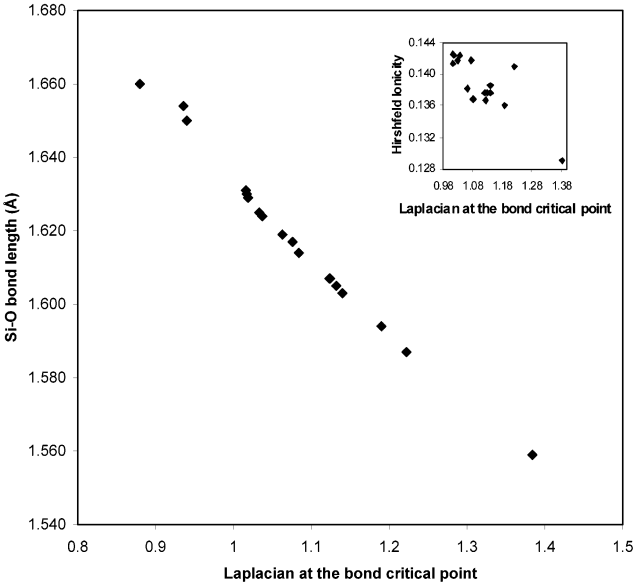

Figure 6. Laplacian at the bond critical point ($\nabla^2\rho_{(rc)}$) vs Si−O bond length (inset shows $\nabla^2\rho_{(rc)}$ vs Hirshfeld ionicity).

employed in each respective set of calculations. It is well-known that for oxygen, especially in anisotropic environments typical for siliceous materials, polarization of the charge density on the oxygen atoms should be allowed for in the basis set.[59] The inclusion of polarization functions in the basis set, describing the oxygen atoms in silica materials is, thus, essential and has been found by us (see Table 3) and others to give a more saturated and accurate description of the oxygen charge distribution. Larin et al.[11,12] did not use such polarization functions, giving rise to doubt over the accuracy of the calculated charges. It should also be noted that, as opposed to our use of experimental crystallographic data for all atoms in the majority of our calculated silica structural fragments, Larin et a*l.*[11,12] used only structures for which the oxygen atom positions were obtained, not from experiment, but from an approximate distance-least-squares procedure.

In an attempt to understand the trends predicted by our calculations, we may imagine the idealized case of an isolated silicon and oxygen atom. Bringing these atoms together will ultimately create a bond between the atoms, but what is less clear in this picture is the relative charge contributions of each atom to the bond. One extreme would be the complete charge transfer from one atom to the other, resulting in an ionic type of interaction, while in the other extreme no charge transfer between the atoms occurs but rather there is a build up of electron density between the atomic nuclei. The comparative measure of ioncity we employ is a simple technique with which to describe the relative degree of atomic charge transfer throughout the range of possible bond types. The simple fact that there is a variation of ionicity with Si−O bond length, for all partitioning methods, indicates that partial atomic charge transfer occurs, showing that the interaction between the atoms is more than purely electrostatic.

The bond lengths of each crystalline silica material included in our study are all slightly shorter than those found in the relaxed-four-ring reference structure, due to them being in a state of natural bulk-induced compression. The range of Si−O bonds to be described is, thus, one of contracted lengths (with respect to the equilibrium distance). Simple electrostatic considerations suggest that shortening the internuclear distance will lead to a progressive deepening of the potential well between the two atoms, increasing the chance of the electron to be found between the atoms rather than close to only one. This crude model for the electron distribution, comparable to the H_2^+ ion, leads to the prediction that ionicity will decrease with decreasing bond lengths as found for both Mulliken and Hirshfeld analyses.

While our simple model of the electron distribution in a heteronuclear bond explains the trends found for both Mulliken and Hirshfeld analyses, it cannot explain the reverse trend as found in Bader analysis. The key to this problem rests in the fundamental differences between the partitioning schemes. Mulliken analysis disregards the details of the topology of the electron density between the two atoms and simply divides it equally between the two atoms. Hirshfeld charges are also relatively insensitive to the details of electron density distribution between the atoms as the method biases its weighted charge density partitioning to the density closest to the respective atomic nuclei. [Although the Hirshfeld atomic charges are relatively stable, the Hirshfeld chemical deformation densities can, however, be sensitive to the choice of reference promolecule on which the weighted charge partitioning is based.[60]] Bader's method on the other hand is very sensitive to the density variations between the atoms, because the partitioning is based upon finding the minima in the electron density ($\nabla\rho = 0$) along the internuclear axis. The effects of polarization of the density between the atoms are, thus, included in the Bader charges, while being neglected in Mulliken and, to a lesser degree, in Hirshfeld charges. This inclusion of polarization though gives, as noted above, rather large integrated atomic charges in the Bader scheme. If these charges were to be interpreted as classical Coulombic atomic-centered charges, silica would be expected to have physical properties characteristic of strongly ionic compounds, e.g., dense closed-packed structures, high atomic-coordination numbers, and a low number of polymorphs which are not observed in siliceous materials.[61,62] This relationship between coordination number and ionicity has been made explicit in both experimental and theoretical studies[5,63] of other materials using as a reference point an ionicity measure, due to Phillips[64] based on a dielectric model of the chemical bond. The Phillips ionicty of α-quartz (0.572[61]) lies between that obtained from Bader and Mulliken charges and is one of the lowest for oxides.[5,63] This relatively low ionicity for silica together with its low coordination is also consistent with the division between high and low coordination compounds based on the Phillips scale.[63,64] While the Phillips ionicity values cannot be used to discriminate between our results based on the different charge analysis schemes, they seem to support the fact that silica has a moderate ionicity, thus indicating further that the obtained Bader ionicities are too high. From a more practical point of view, Mulliken and Hirshfeld methods predict charges which are much more inline with the observed structural properties and are, thus, more suitable than Bader charges for applications in which the electrostatic interactions are modeled as pure point charges, as for instance in the development of force fields.

For silica we have demonstrated that the absolute magnitude of Mulliken-derived atomic charges shows a strong basis set dependency, while Hirshfeld charges are more stable. Furthermore Hirshfeld partitioned atomic charges are known, especially in the multipole expansion, to well reproduce physical observables (molecular dipole moments and electrostatic potential). We, therefore, expect that Hirshfeld charges give a more accurate atomic-charge-based interpretation of the Si−O system. In this respect, it is interesting to note that the Hirshfeld charges, of all the partitioning schemes tested, gives the most covalent description of the Si−O bond.

Our simple model of the heteronuclear bond can now be improved by assuming that the potential well between the atoms is also asymmetric and deeper on the side of the more electronegative element (oxygen). When the internuclear distance is now decreased, the chance of finding an electron between the two atoms rather than close to only one atom is again increased. Furthermore, there is an increased probability of finding an electron in the bond close to the more electronegative element. The model can now explain both the trends for Mulliken and Hirshfeld as well as for Bader analyses. When the bond length is decreased, electron density flows from the atoms into the bond with a bias toward the more electronegative oxygen, thereby lowering the Mulliken and Hirshfeld ionicties and increasing Bader ionicity due to the polarization of the bond.

Our model is further supported by the observation that the Laplacian at the bond-critical point is strongly positive ($\nabla^2\rho_{(rc)} > 0.9$) and increases with decreasing bond length. The strongly positive Laplacian is indicative of the intermediate interaction type (between ionic and covalent) of bonds[27] as can be also found in molecules such as formaldehyde and carbon dioxide. The fact that the Laplacian increases with decreasing bond length is, as with our calculated Bader ionicities, a sign of increasing polarization of the electron density between the atomic nuclei. Furthermore, we find the Hirshfeld ionicty and the Laplacian at the bond critical point to be correlated (see Figure 6) and to be describing the same phenomena as suggested in our model.

In a similar way that individual Si−O bond lengths correlate with the degree of Si−O bond ionicity, there also appears to be an intriguing consistent tendency for the energetic stability of each fragment, and potentially its respective host crystal, to correlate with the *average* Si−O ionicity. Although with our small representative sample of Si−O bonds a strong statistical correlation is not to be expected, the results are suggestive of a tantalising link between global energetic stability of siliceous material frameworks and a fundamental property of the constituent Si−O bonds. Such a link may help to explain the correlations between the measured enthalpy of formation and framework density as observed by Piccione et al.[56] for all-siliceous materials. Further work using larger representative clusters and periodic models are planned to confirm this link.

Conclusions

Our investigation has shown that the cluster approach, using high level DFT calculations and a comparative atomic-charge-based ionicity measure, can give useful insight into the fundamental properties of all-silica materials. In particular, we have shown that the complex procedure of assigning the appropriate description of the Si−O bonds in these materials is largely dependent on the method of charge partitioning analysis employed. The reasons for these differences are discussed, with the degree of polarizability of the oxygen-centered charge density being shown to be particularly important. Irrespective of the diversity in predicted ionicities and charges, we have shown how the trends from each method may be reconciled within a simple model. For a chemically intuitive atomic charge-

based interpretation of the ionicity of siliceous materials Hirshfeld charges are shown to be preferred over Bader and Mulliken charges. Correlations between the individual Si−O bond lengths and individual bond ionicity are observed for all atomic charge partitioning schemes. Our results also suggest that average Si−O ionicity may be linked to the energetic stability of all-siliceous frameworks.

Acknowledgment. This work was sponsored by the stichting Nationale Computerfaciliteiten (National Computing Facilities Foundation, NCF) regarding the use of supercomputer facilities, with financial support from the Nederlandse Organisatie voor Wetenschappelijk Onderzoek (Netherlands Organization for Scientific Research, NWO). We thank N. Ramshaye and Drs. A. A. Sokol and H. van Koningsveld for useful discussions.

References and Notes

(1) van Bekkum, H.; Flanigen, E. M.; Jansen J. C. *Introduction to Zeolite Science and Practice*; Studies in Surface Science and Catalysis 58; Elsevier: Amsterdam, The Netherlands, 1991

(2) Navrotsky, A. *Physics and Chemistry of Earth Materials*; Cambridge University Press: Cambridge, U.K., 1994.

(3) Devine, R. A. B.; Durand, J. P.; Dooryhée, E. *Structure and Imperfections in Amorphous and Crystalline Silicon Dioxide*; Wiley: Chichester, U.K., 2000.

(4) Chulviken, N. D.; Zhidomirov, V. B. *Kinet. Katal.* **1977**, *18*, 903.

(5) Catlow, C. R. A.; Stoneham, A. M. *J. Phys. C: Solid State Phys.* **1983**, *16*, 4321.

(6) Catlow, C. R. A. In *Solid State Chemistry Techniques*; Cheetham, A. K., Day, P., Eds.; Clarendon Press: Oxford, U.K., 1987.

(7) van de Graaf, B.; Njo, S. L.; Smirnov, K. S. In Reviews in Computational Chemistry; Lipkowitz, K. B., Boyd, D. B., Eds.; VCH: New York, 2000; Vol. 14.

(8) Wiberg, K. B.; Rablen, P. R. J. *Comput. Chem.* **1993**, *14*, 1504.

(9) Bachrach, S. M. In *Reviews in Computational Chemistry*; Lipkowitz, K. B., Boyd, D. B., Eds.; VCH: New York, 1994; Vol. 5.

(10) White, J. C.; Hess, A. C. *J. Phys. Chem.* **1993**, *97*, 8703.

(11) Larin, A. V.; Vercauteren, D. P. *Int. J. Inorg. Mater.* **1999**, *1*, 201.

(12) Larin, A. V.; Leherte, L.; Vercauteren, D. P. *Chem. Phys. Lett.* **1998**, *287*, 169.

(13) Pereira, J. C. G.; Catlow, C. R. A.; Price, G. D. *J. Phys. Chem.* **1999**, *103*, 3252.

(14) Kessi, A.; Delley, B. *Int. J. Quantum Chem.* **1998**, *68*, 135.

(15) Elcombe, M. M. *Proc, Phys. Soc.* **1967**, *91*, 946.

(16) Barron, T. H. K.; Huang, C. C.; Pasternak, A. *J. Phys. C* **1976**, *9*, 3925.

(17) Striefler, M. E.; Barsch, G. R. *Phys. Rev. B* **1975**, *12*, 4553.

(18) Smirnov, K. S.; van de Graaf, B. *J. Chem. Soc., Faraday Trans.* **1996**, *92*, 2475.

(19) Pantelides, S. T.; Harrison, W. A. *Phys. Rev. B* **1976**, *13*, 2667.

(20) Sauer, J. *Chem. Rev.* **1989**, *89*, 199.

(21) Boronat, M.; Zicovich-Wilson, C. M.; Corma, A.; Viruela, P. *Phys. Chem. Chem. Phys.* **1999**, *1*, 537.

(22) Lopez, N.; Pacchioni, G.; Maseras F.; Illas F. *Chem. Phys. Lett.* **1998**, *294*, 611.

(23) Mulliken, R. S. *J. Chem. Phys.* **1955**, *23*, 1833.

(24) Hirshfeld, F. L. *Theor. Chim. Acta* (*Berlin*) **1977**, *44*, 129.

(25) Rousseau, B.; Peeters, A.; Van Alsenoy, C. *Chem. Phys. Lett.* **2000**, *324*, 189.

(26) Nalewajski, R. F.; Parr, R. G. *Proc. Natl. Acad. Sci. U.S.A.* **2000**, *97*, 8897.

(27) Bader, R. F. W. *Atoms in Molecules−A Quantum Theory*; Oxford University Press: Oxford, U.K., 1990.

(28) Vitiello, M.; Lopez, N.; Illas, F.; Pacchioni, G. *J. Phys. Chem. A* **2000**, *104*, 4674.

(29) Teunissen, E. H.; Roetti, C.; Pisani, C.; de Man, A. J. M.; Jansen, A. P. J.; Orlando, R.; van Santen, R. A.; Dovesi, R. *Model. Simulation Mater. Sci. Eng.* **1994**, *2*, 921.

(30) Shah, R.; Gale, J. D.; Payne, M. C. *J. Phys. Chem B* **1997**, *101*, 4787.

(31) Mihaleva, V. V.; van Santen, R. A.; Jansen A. P. J. *J. Phys. Chem. B* **2001**, *105*, 6874.

(32) Ricci, D.; Pacchioni, G.; Szymanksi, M. A.; Shluger, A. L.; Stoneham, A. M. *Phys. Rev. B* **2001**, *64*, article no. 224104.

(33) Greatbanks, S. P.; Hillier, I. H.; Burton, N. A.; Sherwood, P. *J. Chem. Phys.* **1996**, *105*, 3770.

(34) Sauer, J.; Sierka, M. *J. Comput. Chem.* **2000**, *21*, 1470.

(35) Diaz-Cabañas, M. J.; Barrett, P. A.; Camblor, M. A. *Chem. Commun.* **1998**, 1881.

(36) Hriljac, J. J.; Eddy, M. M.; Cheetham, A. K.; Donohue, J. A.; Ray, G. J. *J. Solid State Chem.* **1993**, *106*, 66.

(37) Barrett, P. A.; Camblor, M. A.; Corma, A.; Jones, R. H.; Villaescusa, L. A. *Chem. Mater.* **1997**, *9*, 1713.

(38) Villaescusa, L. A.; Barret, P. A.; Camblor, M. A. *Angew. Chem., Int. ed.* **1999**, *38*, 1997.

(39) Camblor, M. A.; Corma, A.; Lightfoot, P.; Villaescusa, L. A.; Wright, P. A. *Angew. Chem., Int. ed.* **1997**, *36*, 2659.

(40) Fyfe, C. A.; Gies, H.; Kokatailo, G. T.; Marler, B.; Cox, D. E. *J. Phys. Chem.* **1990**, *94*, 3718.

(41) Marler, B.; Grünewald-Lüke, A.; Gies, H. *Microporous Mesoporous Mater.* **1998**, *26*, 49.

(42) Araki, T.; Zoltai, T. Z. *Kristallografiya* **1969**, *129*, 381.

(43) Heaney, P. J.; Post, J. E. *Am. Mineral.* **2001**, *86*, 1358.

(44) Becke, A. D. *J. Chem. Phys.* **1993**, *98*, 5648.

(45) Lee, C.; Yang, W.; Parr, R. G. *Phys. Rev. B* **1988**, *37*, 785.

(46) Frisch, M. J.; Trucks, G. W.; Schlegel, H. B.; Scuseria, G. E.; Robb, M. A.; Cheeseman, J. R.; Zakrzewski, V. G.; Montgomery, J. A., Jr.; Stratmann, R. E.; Burant, J. C.; Dapprich, S.; Millam, J. M.; Daniels, A. D.; Kudin, K. N.; Strain, M. C.; Farkas, O.; Tomasi, J.; Barone, V.; Cossi, M.; Cammi, R.; Mennucci, B.; Pomelli, C.; Adamo, C.; Clifford, S.; Ochterski, J.; Petersson, G. A.; Ayala, P. Y.; Cui, Q.; Morokuma, K.; Malick, D. K.; Rabuck, A. D.; Raghavachari, K.; Foresman, J. B.; Cioslowski, J.; Ortiz, J. V.; Baboul, A. G.; Stefanov, B. B.; Liu, G.; Liashenko, A.; Piskorz, P.; Komaromi, I.; Gomperts, R.; Martin, R. L.; Fox, D. J.; Keith, T.; Al-Laham, M. A.; Peng, C. Y.; Nanayakkara, A.; Gonzalez, C.; Challacombe, M.; Gill, P. M. W.; Johnson, B. G.; Chen, W.; Wong, M. W.; Andres, J. L.; Head-Gordon, M.; Replogle E. S.; Pople, J. A. *Gaussian 98*, revison A.9; Gaussian, Inc.: Pittsburgh, PA, 1998.

(47) Binkly, J. S.; Pople, J. A.; Hehre, W. J. *J. Am. Chem. Soc.* **1980**, *102*, 939.

(48) Gordon, M. S.; Binkley, J. S.; Pople, J. A.; Pietro, W. J.; Hehre, W. J. *J. Am. Chem. Soc.* **1982**, *104*, 2797.

(49) Dobbs, K. D.; Hehre, W. J. *J. Comput. Chem.* **1986**, *7*, 359.

(50) Dobbs, K. D.; Hehre, W. J. *J. Comput. Chem.* **1987**, *8*, 861.

(51) Dobbs, K. D.; Hehre, W. J. *J. Comput. Chem.* **1987**, *8*, 880.

(52) *AIM2000*, version 1.0; University of Applied Sciences: Bielfeld, 1998.

(53) Catlow, C. R. A.; Freeman, C. M.; Islam, M. S.; Jackson, R. A.; Leslie, M.; Tomlinson, S. H. *Philos. Mag. A* **1988**, *58*, 123.

(54) Hammonds, K. D.; Heine, V.; Dove, M. T. *J. Phys. Chem. B* **1998**, *102*, 1759.

(55) Hobbs, W.; Jeresum, C. E.; Pulim, V.; Berger, B. *Philos. Mag. A* **1998**, *78*, 679.

(56) Piccione, P. M.; Laberty, C.; Yang, S.; Camblor, M. A.; Navrotsky, A.; Davis, M. E. *J. Phys. Chem. B* **2000**, *104*, 10001.

(57) Silvi, B.; Savin, A.; Wagner, R. F. In *Modelling of Minerals and Silicated Materials*; Silvi, B., D'Arco, P., Eds.; Kluwer Academic Publishers: Dordrecht, The Netherlands, 1997.

(58) Gibbs, G. V.; Hill, F. C.; Boisen, M. B., Jr. In *Modelling of Minerals and Silicated Materials*; Silvi, B., D'Arco, P., Eds.; Kluwer Academic Publishers: Dordrecht, The Netherlands, 1997.

(59) Nedelec, J. M.; Hench, L. L. *J. Non-Cryst. Solids* **2000**, *277*, 106.

(60) Schwarz, W. H. E.; Ruedenberg, K.; Mensching, L. *J. Am. Chem. Soc.* **1989**, *111*, 6926.

(61) Engel, G. F.; Defregger, S. *Phys. Status Solidi B* **1991**, *163*, 389.

(62) Lucovsky, G. *J. Non-Cryst. Solids* **2002**, *303*, 40.

(63) Christensen, N. E.; Satpathy, S.; Pawlowska, Z. *Phys. Rev. B* **1987**, *36*, 1032.

(64) Phillips, J. C. *Rev. Mod. Phys.* **1970**, *42*, 317.